Journal of the Korean Nuclear Society
Volume 29, Number 2, pp. 138~147, April 1997

Flare Test and Stress Analysis of Alloy 600/690 Tubes

W.G. Kim, J. Jang, and I.H. Kuk
Korea Atomic Energy Research Institute
150 Dukjin-dong, Yusong-gu, Taejon 305-353, Korea

(Received July 5, 1996)

Abstract

Korean-made alloys 600 and 690 tubes were evaluated by flare tests according to ASTM standards, and acting stresses during the test were analyzed. All the tubes, including alloys 600 and 690 tubes with various heat treatment conditions, satisfied the requirement with 30 or 35% O.D expansion. Axial stresses in alloy 690 tubes were higher than those in alloy 600 ones and the gap increased gradually with flaring percentage(F.P, %). Assuming the tubes as the rigid-perfectly plastic body, a stress equation was obtained using modified Tresca's yield criterion. Also microstructural change of the flared tubes was discussed with the acting stresses.

1. Introduction

Alloys 600 and 690 with various heat treatment conditions have been widely used as steam generator tubes. For alloy 600 many research works have been conducted to improve the corrosion resistance and partly succeeded the goal and the special heat treatment technique has been adapted for some duration[1-4]. Recently alloy 690, due to its superior corrosion resistance to alloy 600, is taking over alloy 600 for replaced or new steam generator[5-10].

In the assembly of steam generators, U-shaped tubes are fixed in the tube sheet with the support from tube support plates and ends of the tubes are expanded in the holes of tube sheet by one of various methods. Stress state during the expansion process changes with the degree of expansion and along the position within tubes, i. e., tensile stress in the expanded region, compressive stress in the un-expanded region and tensile-to-compressive in the transition region. Stress is one of important factors to stress corrosion cracking(SCC) and especially residual stress introduced after any processings can contribute to the stress corrosion cracking behavior of the tubes. Residual stresses after other processings could be removed by heat treatment, but not after the tube expansion, because this is one of the last procedures in the steam generator assembly[11-13]. Any minor cracks can initiate failure under operating conditions of high temperature and pressure in nuclear power plant. Therefore tube suppliers have to show that tube expansion procedure does not develop any minor cracks in the tubes[14].

In this study Korean-made alloys 600 and 690 tubes were evaluated by flare tests and acting stresses during the test were analyzed. Stress equation for the flare test was obtained using modified Tresca's criterion and stresses during the test were calculated for 600 and 690 tubes. Mechanical properties from over-all tube tensile test were used in the analysis. Microstructural changes after the flare test were observed and discussed with the acting stresses.

2. Background Theory of Flare Test of Thin-Wall Tubes

Cylinders or tubes are classified as thick or thin ones according to the ratio of thickness to diameter, t/D. When t/D is larger than 0.1, it is called as thick one and when smaller than 0.1, as thin. In the case of domestic steam generator, tube outer diameter (O.D) is 19.05 mm and wall thickness is about 1.05 mm. So we can treat them as thin ones[15] and can thus assume insignificantly the variation in stress across the wall of the tube.

Figure 1(a) shows schematic tube section during flare test with conical plug of semisolid angle of α. Tube with initial diameter $D_1(=2R_1)$ is flared by a conical plug until diameter becomes $D_2(=2R_2)$. Each element within tubes is under quasi-static state during the flare test. Acting stresses at the any mean radius of r are shown in Figure 1(b).

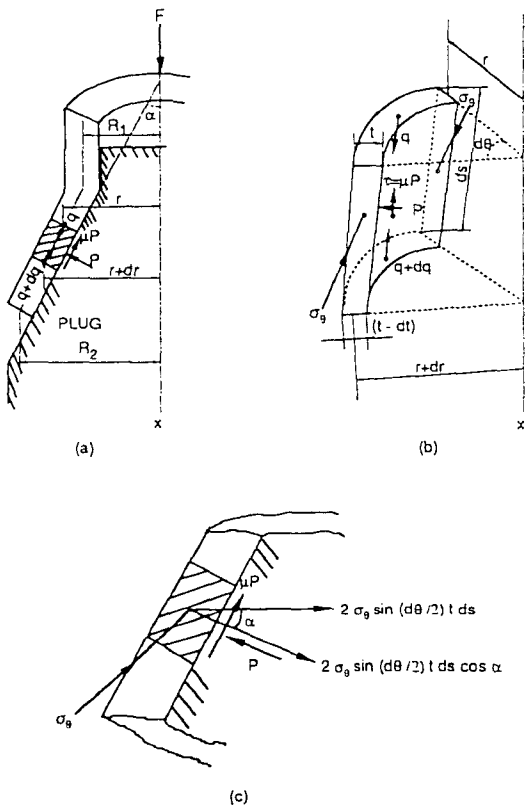

Fig. 1.(a) Schematic Diagram on the Tube Flaring with Conical Plug, 60° Angle.
(b) Stresses Acting on an the Small Fragmentary Element of the Tube.
(c) Component of the Radial Force due to the Hoop Stress, σ_θ, Exerted on an Element in a Direction Normal to the Plug.

where q : axial stress, parallel to the plug face
σ_θ : hoop stress
p : pressure perpendicular to wall thickness
$\tau=\mu p$: frictional stress between tube and plug
μ : friction coefficient
t : wall thickness at any mean radius of r
ds : length of an element parallel to plug face

The radial component of the force exerted on the element due to the hoop stress σ_θ, is $2\,\sigma_\theta \sin(d_\theta/2)\, t\, ds$, which has a component normal to the plug face as shown in Figure 1(c).

Resolving forces exerted on the element in a direction normal to the plug face,

$$p\,r\,d\theta\,ds - 2\,\sigma_\theta \sin(d\theta/2)\,t\,ds\cos\alpha = 0 \qquad (1)$$

since $\sin d\theta \doteq d\theta$,

$$p\,r\,d\theta\,ds - \sigma_\theta\,d\theta\,t\,ds\cos\alpha = 0$$

$$p = \sigma_\theta\, t\cos\alpha / r \qquad (2)$$

Resolving forces exerted on the element in a direction parallel to the plug face

$$(q+dq)(r+dr)\,(t-dt)\,d\theta - q\,r\,d\,d\theta +$$

$$2\sigma_\theta \sin(d\theta/2)\,t\,ds\,\sin\alpha + \mu p\,r\,d\theta\,ds = 0 \qquad (3)$$

Neglecting the second derivatives, and dividing by $(d\theta\, dr)$

$$rt\left(\frac{dq}{dr}\right) + qt\left(\frac{dr}{dr}\right) - qr\left(\frac{dt}{dr}\right) +$$

$$\sigma_\theta t + \mu p r\left(\frac{1}{\sin\alpha}\right) = 0 \qquad (4)$$

Combining the eqn (2) and (4), we obtain the equilibrium differential equation for tube flaring

$$rt\left(\frac{dq}{dr}\right) + qt\left(\frac{dr}{dr}\right) - qr\left(\frac{dt}{dr}\right) +$$

$$\sigma_\theta t + \mu\sigma_\theta t\cot\alpha = 0 \qquad (5)$$

Assuming constant wall thickness during the process, $dt/dr \rightarrow 0$, equation (5) becomes

$$r\left(\frac{dq}{dr}\right) + q + \sigma_\theta(1 + \mu\cot\alpha) = 0$$

$$r\left(\frac{dq}{dr}\right) + q + \sigma_\theta(1 + B) = 0 \qquad (6)$$

where $B = \mu \cot \alpha$. Since $t \cos(\alpha/r)$ is negligible in the case of thin tube, the normal plug pressure p, is smaller than circumferential one. Hence, σ_θ(tensile) $\geq$ p $\geq$ q (compressive) or 1 = σ_1, $\sigma_2 = p$ and σ_3 = q. Von Mises' criterion gives $\sigma_1^2 - \sigma_1\sigma_3 + \sigma_3^2 = Y^2$. For the same stress state, the Tresca's yield criterion gives $\sigma_1 - \sigma_3 = Y$. Von Mises' yield criterion is good for the yield phenomena of most metals, but Tresca's criterion is more convenient when the magnitude and directions principal stresses are known [10]. In this study we use modified Tresca's yield criterion, *i. e.*,

$$\sigma_1 - \sigma_3 = m\ Y \qquad (7)$$

when m is a constant derived by the method of least squares and has the approximate value of 1.08. Modified Tresca's yield criterion is

$$\sigma_\theta - (-q) = m\bar{Y} \qquad (8)$$

or

$$\sigma_\theta = m\bar{Y} - q \qquad (9)$$

where $\bar{Y}$ is average yield stress. Combining eqn (6) and (9)

or $$r\left(\frac{dq}{dr}\right) + q + (m\bar{Y} - q)(1 + B) = 0$$

Therefore $$r\left(\frac{dq}{dr}\right) + Bq + m\bar{Y}(1 + B) = 0$$

$$\frac{dq}{[Bq - m\bar{Y}(1 + B)]} = \frac{dr}{r} \qquad (10)$$

Integrating(10), $\left(\frac{1}{B}\right)\ln(Bq + C) = \ln r + \ln A$,

where $\ln A$ is integral constant,

$$C = -\ m\ Y\ (\ 1\ +\ B\ )$$

$$(Bq+C)^{1/B} = r\ A$$

At the entrance to the plug (where r = $D_1/2$), $q_1 = 0$

$$C^{1/B} = R_1\ A \quad \text{or} \quad A = C^{1/B}/\ R_1$$

$$(\ Bq\ +\ C\ )^{1/B} = (\ r/R_1\ )\ C^{1/B}$$

$$Bq\ +\ C = (\ r/R_1\ )^B\ C$$

Therefore, axial stress becomes

$$q = (\ C/B\ )\ [\ (r/R_1)^B\ -\ 1\ ]$$

$$q = m\bar{Y}\ [(1+B)/B]\ [1-(r/R_1)^B\ ] \qquad (11)$$

At the other end of the plug, where $r = D_2/2$, axial stress, q_2, becomes

$$q_2 = m\bar{Y}\ [(1+B)/B\ ]\ [1-(R_2/R_1)^B\ ]$$

$$q_2 = m\bar{Y}\ [(1+B)/B\ ]\ [1-(D_2/D_1)^B\ ] \qquad (12)$$

Hoop stress, θ, can be obtained using equation (9) and axial stress from equation (11).

Axial force ,F, is thus given by $F \approx q_2(\pi D_2 t/\cos\alpha)$

$$F \approx (\pi D_2 t/\cos\alpha)\, m\bar{Y}\ [(1+B)/B\ ][1-(D_2/D_1)^B\ ] \qquad (13)$$

3. Experiment

Six different tubes were flare tested; K600-MA, K600-TT, and I600-MA, K690-MA, K690-TT, and I690-MA. Series K were prepared by Sammi Special Steel Co. from alloy melting to mill annealing. Series I were manufactured using INCO's forged bar. MA series are just mill annealed(1040℃/15min) ones and TT series are vacuum heat treated (710℃/15hr) ones after mill annealing.

Chemical composition of the tubes are shown in Table 1. All the elements are well with the required composition range, but carbon contents in K tubes are revealed as a little lower.

Tensile test specimens were prepared for over-all tube test following ASTM standard[17]. Tube length was 300mm and two 100 mm long steel plugs were inserted in both ends of the tube. Gauge length was 70 mm and strain rate was around 2×10^{-3}/sec. Yield strength of 0.2% off set values was measured.

Table 1. Chemical Compositions of Alloy 600 and 690 Tubes (wt%)

	Ni	Cr	C	Mn	Al	Fe	Co	S
K600	74.5	15.6	0.016	0.21	0.13	7.2	0.03	<0.001
K690	64.2	27.7	0.014	0.23	0.24	8.1	0.12	<0.001
I600	74.2	15.3	0.031	0.23	0.22	8.6	0.05	<0.001
I690	62.6	28.0	0.020	0.08	0.35	9.2	0.12	<0.001

I : INCO-made Tube K : Korean-made Tube

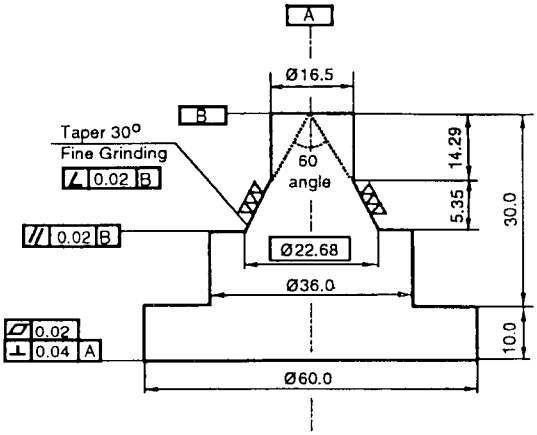

Fig. 2. Schematic Diagram of Jig for Flare Test of Tubes.

Tube samples for flare test were prepared as 50mm in length and the both ends of the tubes were machined very slowly with lubricant to avoid any work hardening effect.

According to ASTM standards on flaring tests (B163-86a)[14], an expanding tool was prepared with an included angle of 60°. The expanding tool (conical plug) was fabricated with SKD-11 steel, of which surface was hardened by heat treatment. Schematic drawing of expanding tool is shown in Figure 2. Tubes were expanded by compression with the expanding tools until outside diameter of the tubes increased by 30%. Expanded tubes were visually inspected after the flare tests.

Flare test was done using universal tester with 1×10^{-3}/sec strain rate at room temperature. Microstructural change was observed after flare test applying usual metallographic preparation and electrolytic etching with 5% nital solution.

4. Result and Discussion

4.1 Flare Test

Table 2 shows the whole tube tensile test results. Tensile and yield strength of alloy 690 tubes are all higher than those of alloy 600 ones, but elongations are similar. After TT processing (thermal treated at 710℃ for 15hr in vacuum after mill annealing) yield strength decreases, but not the tensile strength.

No minor crack was found after flare tests with 30% or even with 35% O.D expansion for all tubes. Thus, all the tubes were evaluated as good in the viewpoint of flaring behavior. Specimens after 30% and 35% O.D expansion were shown in Figure 3.

Figure 4 shows applied force-flare percentage (F. P,%) flow curves. The flaring percentage (F.P, %) is

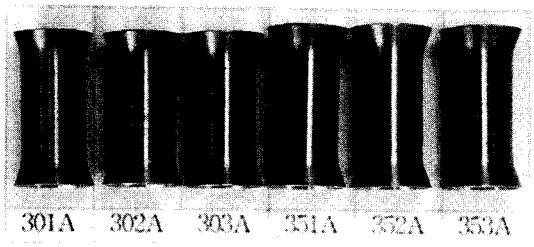

Fig. 3. 30% and 35% O.D Flared Tested Tubes.

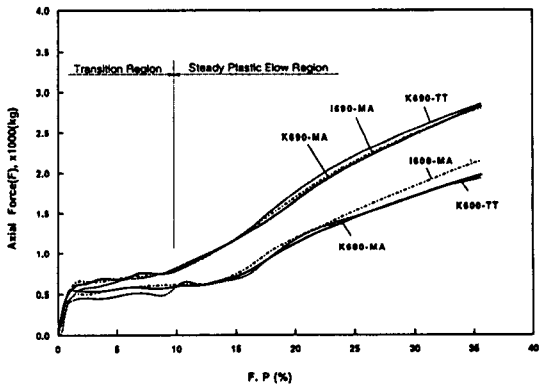

Fig. 4. Flow Curves on Various Alloy 600 and 690 Tubes by Flare Test.

presented as a function of the variation of tube diameter. As flare percentage increases the applied force increases. More force was needed for alloy 690 tube than for alloy 600 at same flare percentage(%)

Table 2. Mechanical Properties of Alloy 600 and 690 Tubes

Specimens		Thermal Condition	YS(MPa) (0.2% Offset)	TS(MPa)	Elongation (%)
MA	K600-MA	1040℃/15min	407	698	34
	I600-MA	1040℃/15min	382	735	36
	K690-MA	1040℃/15min	412	792	38
	I690-MA	1040℃/15min	450	785	37
TT	K600-TT	MA+710℃/15hr	340	696	36
	K690-TT	MA+710℃/15hr	380	791	38

*MA : Mill Annealed TT : Thermally Treated
I : INCO-made Tube K : Korean-made Tube

because alloy 690 contains more Cr and alloy 690 tubes shows higher work hardening effect than alloy 600 one. Tensile strength and elongation of alloy 690 tubes were similar with those of alloy 600 respectively, but yield strength shows much higher than alloy 600 (Table 2).

Figure 5 shows the microstructures before flare test of alloy 600 and 690 MA tubes. In case of alloy 690 tubes (c,d) many twin faces are observed in grains, and carbide precipitations are distributed along grain boundaries. Figure 6 shows microstructures of alloy 600 tubes after 35% O.D expansion flare test. Figure 6 (a) and (c) shows grains elongated by hoop stress, and (b) and (d) shows axial section of O.D surface and no significant morphological change. Figure 7

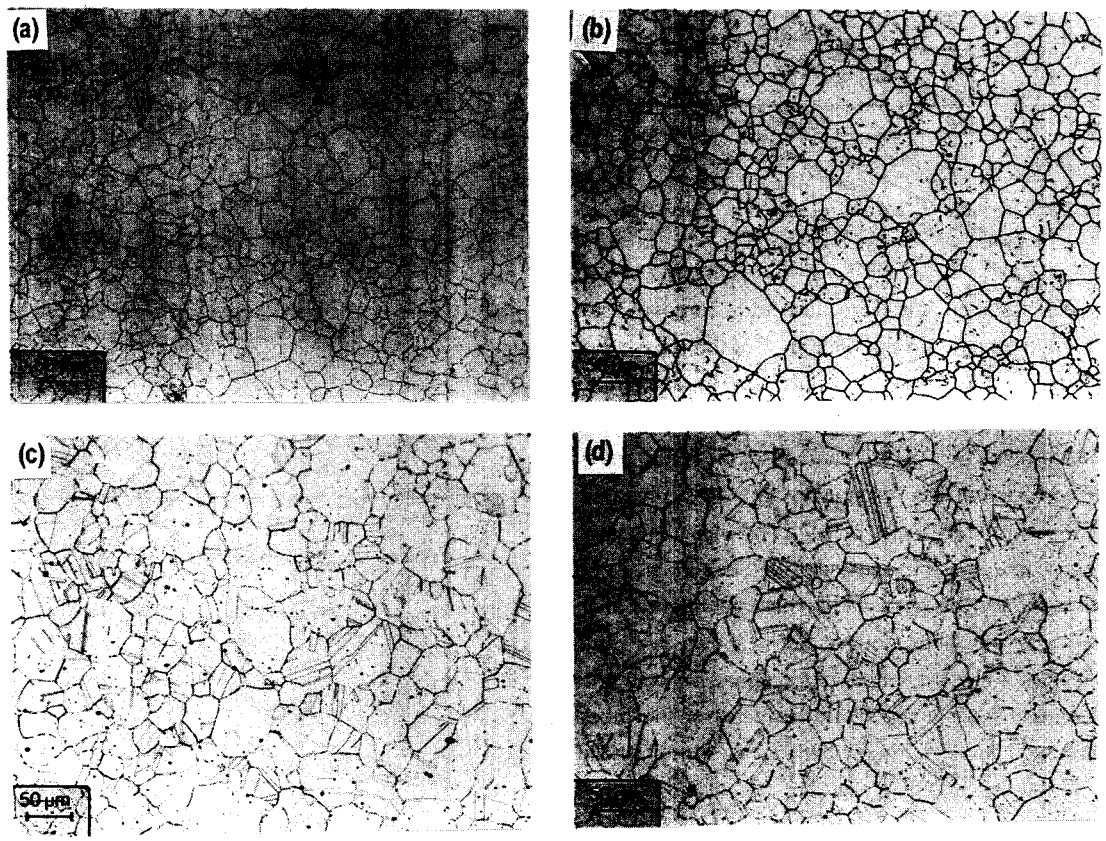

Fig. 5. Optical Microstructure before the Flare Test of Mill Annealed Tubes; (a)K600-MA, (b)I600-MA, (c) K690-MA, (d) I690-MA. (K : Korean-made Alloy Tubes, I : INCO Alloy Tubes)

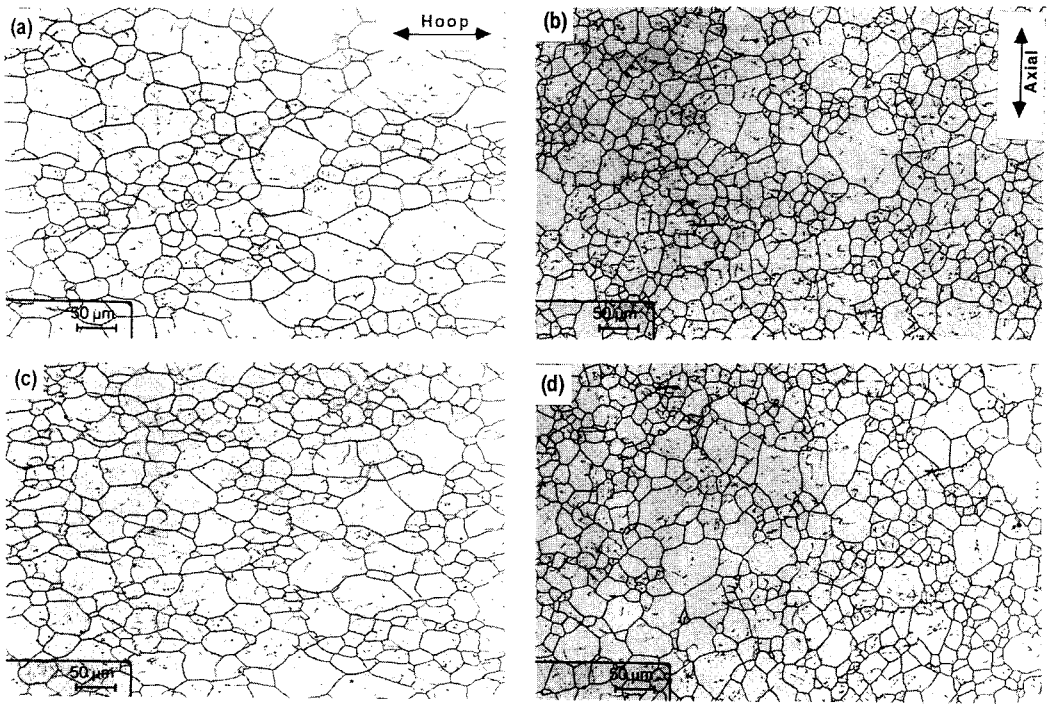

Fig. 6. Optical Microstructure Showing Hoop(a),(c) and Axial(b),(d) Direction Deformation after Flare Tested Alloy 600 Tubes. ((a),(b) : K600-MA Tube, (c),(d) : I600-MA Tube)

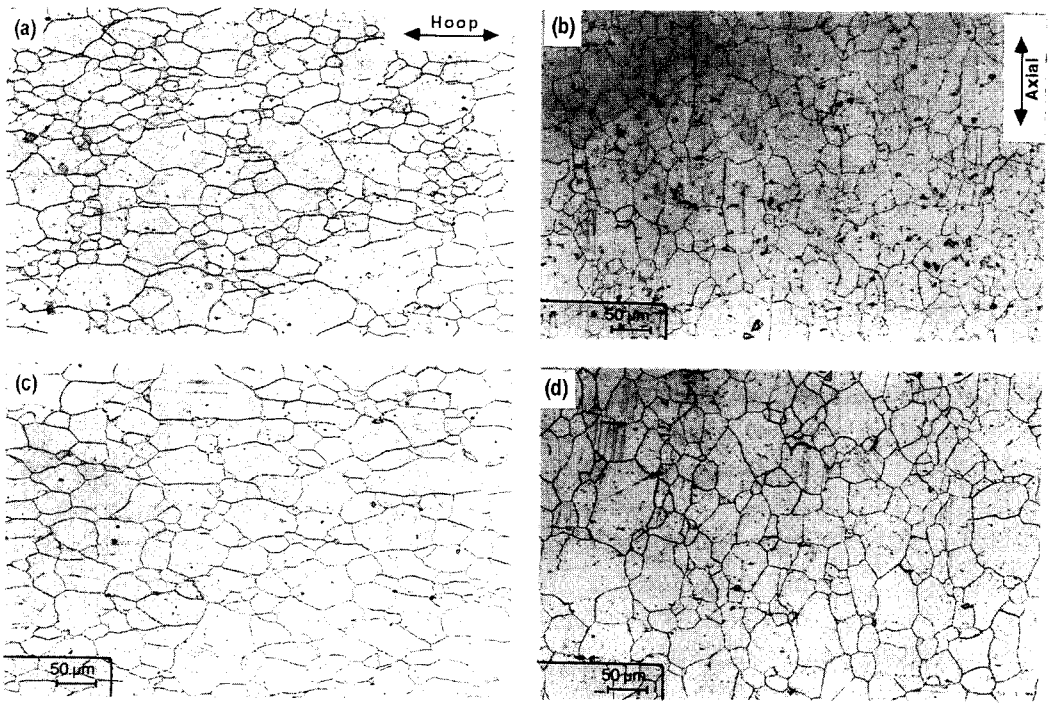

Fig. 7. Optical Microstructure Showing Hoop(a),(c) and Axial(b),(d) Direction Deformation after Flare Tested Alloy 690-TT Tubes. ((a),(b) : K690-TT Tube, (c),(d) : I690-TT Tube)

shows the microstructure of 35% O.D expansion flare tested alloy 690 tubes. Figure 7 (a) and (c) shows clearly that grains are elongated along tube hoop direction like in alloy 600 tubes. Therefore, Hoop stress, σ_θ was more dominant than axial stress, q

4.2 Stress Analysis

Rigid perfectly-plastic body was assumed for the analysis of flow curve. Acting stresses σ_θ, q, F during flare test were calculated using eqn (9), (12), and (13). Friction coefficient μ, constant m, were assumed as 0.2 and 1.08, respectively. Semisolid angle of plug, α, was 30°. Values from Table 2 were used for yield strength, Y, and wall thickness change during the test was neglected.

Calculated values of σ_θ and q in alloy 600 tubes are shown Figs 8 and 9, respectively. Hoop stress, σ_θ, increases almost linearly with flare percentage (%), however axial stress, q, shows negative(−) value, *i. e.*, compressive stress, with some deviations among tubes (Figure 9). The slope is highest in K600-MA tube and lowest in K600-TT.

Table 3 shows the calculated values of σ_θ, q, F in 30% O.D expanded alloy 600 tubes. Again σ_θ is highest (61.27 kg/mm^2) in K600-MA tube and lowest (51.23 kg/mm^2) in K600−TT one. Axial stress, q, is largest (−16.45 kg/mm^2) in K600-MA tube and smallest (−13.76 kg/mmσ^2) in K600-TT one. Therefore the acting stresses in tube element during the flare test are different with heat treatment conditions (MA or TT).

Figure 10 illustrates the calculated and the measured values of axial compressive force, F, during the tests of alloy 600 tubes. The calculated values for K600-MA tube are very close to the measured one after the transition region of about 10% expansion. And K600-TT tube shows a little gap between the measured and calculated values because of additional thermal treatments; *i. e*, YS values of TT tubes was reduced to 340(MPa) from 407(MPa) of MA tubes, and UTS values between two materials does not have difference, as of 696 and 698(MPa).

Table 2. Flaring Stress on Alloy 600 in 30% O. D expansion tubes

	σ_θ(kg/mm^2)	q (kg/mm^2)	F (kg)
K600-MA	61.27	−16.45	−1431.28
I600-MA	57.46	−15.46	−1345.06
K600-TT	51.23	−13.76	−1196.75

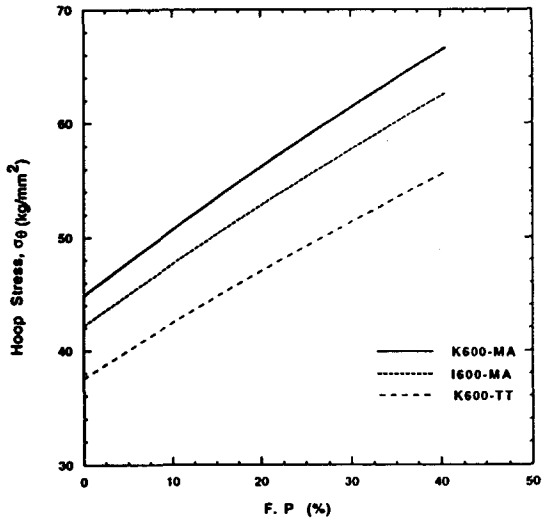

Fig. 8. Hoop Stress Analysis with F.P(%) on Alloy 600 Tubes.

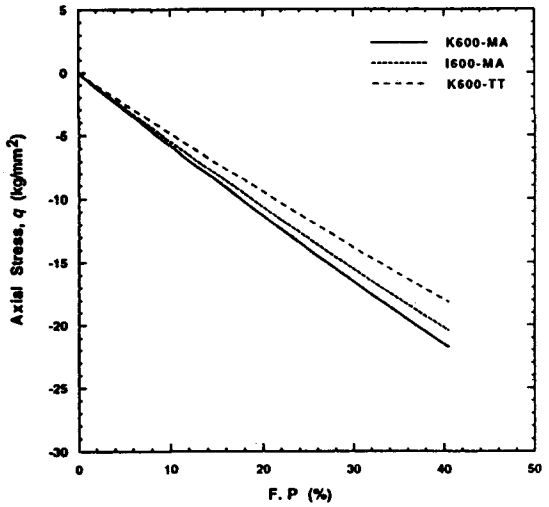

Fig. 9. Axial Stress Analysis with F.P(%) on Alloy 600 Tubes.

Thus two curves between 600 TT tubes may differ with a little gap due to YS values.

On the other hand alloy 690 tubes showed a large gap between the measured and calculated values, as shown in Figure 11. The measured values showed higher than the calculated ones, and the gap between the two widen with flaring percentage(%). Larger gaps in flow curves of TT tubes than MA ones seem to be mainly attributed to the stress relief

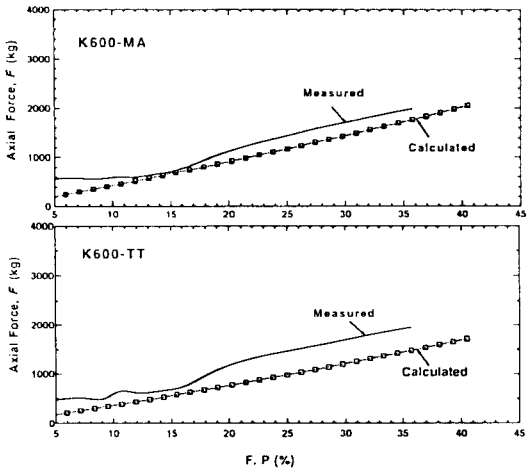

Fig. 10. Comparision of Calculated and Measured Flow Curves on K600-MA and K600-TT Tubes with F. P(%).

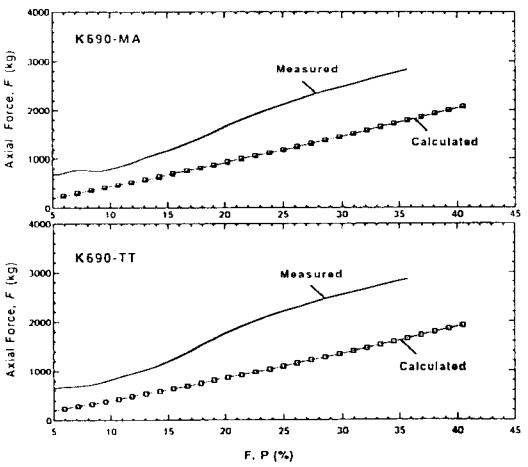

Fig. 11. Comparision of Calculated and Measured Flow Curves on K690-MA and K690-TT Tubes with F.P(%).

effect following more precipitation of chromium carbide along grain boundary, as shown in Figure 12(a, b). After TT treatment carbide precipitate density becomes higher. However, it seems to influence the mechanical properties (including flaring behavior) by stress relief effect due to further decrease of dislocations and the supersaturated solid solution hardening element (e. g. chromium) rather than carbide morphology itself although the main goal of TT treatment is not the stress relieving.

In addition, the increasing of difference gaps of alloy 690 tubes with flaring percentage increases seems to attribute to higher Cr contents, which may cause more work hardening effects due to twin boundary, as shown in Figure 7(b,d). Consequently, whether

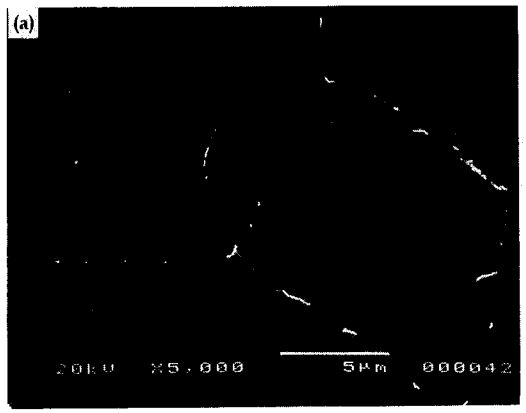

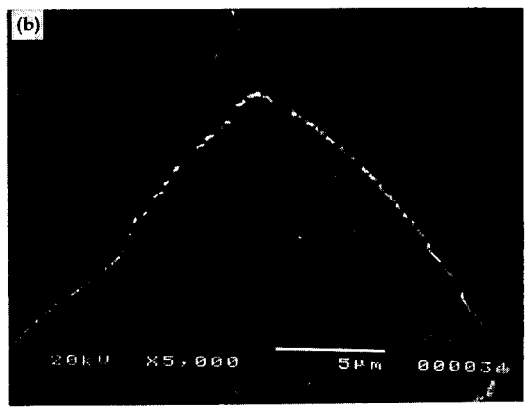

Fig. 12. Scanning Electron Micrographs of (a) K690-MA and (b) K690-TT tubes. (etchant; Bromine-Methanol Solution)

theoretically obtained equations agreed with measured values or not, it depends on material parameters; alloy 600 or 690, and MA or TT.

5. Conclusions

All the alloys 600 and 690 tubes met with the ASTM flare test requirements which no minor cracks was found until 30% and 35% O.D expansion. Flow curves measured during flare tests were steeper in 690 tubes than those in 600 ones and the gap increased gradually with flaring percentage(F.P, %). Calculated stresses, using modified Tresca's yield criterion, during flare test agreed well with the measured ones for alloy 600 tubes, but deviated from the measured ones for alloy 690 tubes. This behavior seems to be attributed to the large chromium content in alloy 690 and the bigger solid solution hardening effect. Flow curves between calculated and measured values depend on material parameters; alloy 600 or 690, and MA or TT. In case of alloy 600 tubes, it became possible to predict the mount of acting stresses within tubes during expansion processes using derived equations.

References

1. D.L. Harrod, et al., "The Temperature Depedenance of Tensile Properties of Thermally Treated Alloy 690 Tubing", *Fifth International Symposium on Environmental Degradation of Materials in Nuclear Power Systems-Water Reactors*, pp849-854, Aug. 25-29 (1991)
2. F. Cattant, et al., "Effectiveness of 700℃ Thermally Treatment on Primary Water Stress Corrosion Sensitivity of 600 Steam Generator Tubes : Laboratory Tests and in Field Experience", *Fifth International Symposium on Environmental Degradation of Materials in Nuclear Power Systems-Water Reactors*, pp901-913, Aug. 25-29 (1991)
3. G.P. Airey, "Optimization of Metallurgical Variables to Improve the Stress Corrosion Resistance of Inconel 600", *EPRI NP-1354*, March (1980)
4. W.C. Kim, et al., "Studies Related to the Secondary-Side SCC Evaluations in Steam Generator Tubes of Nuclear Power Plants", *KAERI/RR-765/88*, pp84-87, December (1988)
5. H. Widmark, "Materials for the Nuclear Power Industry", *Sandvik Steel*, November (1986)
6. W.S. Ryu, "Study on Thermal & Mechanical Properties of U-Tube Material for Steam Generator, *KAERI/RR-1990/92*, December (1992)
7. Cebelcor, "Steam Generator Corrosion Studies", *EPRI NP-2331*, April (1982)
8. G.J. Theus, "Stress Corrosion Cracking of 600 and Alloy 690 in All Volite Treated Water at Elevated Temperatures", *EPRI NP-3061*, May (1983)
9. J.F. Newman, "Stress Corrosion of Alloy 600 and 690 in Acidic Sulfate Solutions at Elevated Temperatures", *EPRI NP-3043*, October (1983)
10. A. Smith, et al., "Relationship between Composition, Microstructure and Corrosion Behavior of Alloy 690 Steam Generator Tubing for PWR Systems", *Fourth International Symposium on Environmental Degradation of Materials in Nuclear Power Systems-Water Reactors*, pp33-46 Aug. (1989)
11. R. McGregor, et al., "Experimental Residual Stress Evaluation of Hydraulic Expansion Transitions in Alloy 690 Steam Generator Tubing", *Seventh International Symposium on Environmental Degradation of Materials in Nuclear Power Systems-Water Reactors*, pp495-507, Vol. 1, Aug. 7-10 (1995)
12. J. Woodward, et al., "Stress Relief to Prevent Stress Corrosion in the Transition Region of Expanded Alloy 600 Steam Generator Tubing", *EPRI NP-3055*, May (1983)
13. G.V. Amoruso, et al., "Stress Corrosion Cracking Test of Expanded Steam Generator Tubes", *EPRI-NP5012*, January (1987)

14. ASTM, "Standard Specification for Seamless Nickel and Nickel Alloy Condenser and Heat Exchanger Tubes", *ASTM Designation B163-86a*, pp62-63, March (1986)
15. M.F. Spotts, "Mechanical Design Analysis", *Engle Cliffs, New Jersey*, pp122-123, (1964)
16. R.A.C. Slater, "Engineering Plasticity-Theory and Application to Metal Forming Process", *John Wiley-New York*, pp296-301, (1977)
17. ASTM, "Standard Test Methods of Tension Testing of Metallic Materials", *ASTM Designation E8-87a*, pp121-134, May (1988)